

Cite this: *Chem. Sci.*, 2023, 14, 7905

All publication charges for this article have been paid for by the Royal Society of Chemistry

Received 30th March 2023  
Accepted 13th June 2023

DOI: 10.1039/d3sc01656k

rsc.li/chemical-science

# Enantioselective synthesis of hydantoins by chiral acid-catalysed condensation of glyoxals and ureas†

Sushant Aryal,<sup>a</sup> Christopher A. Hone,<sup>b</sup> Matthew I. J. Polson<sup>a</sup> and Daniel J. Foley<sup>a,c</sup>

Hydantoins are important scaffolds in natural products and pharmaceuticals, with only a few synthetic strategies available for their asymmetric preparation. We herein describe a single-step enantioselective synthesis of 5-monosubstituted hydantoins *via* condensation of glyoxals and ureas in the presence of a chiral phosphoric acid at room temperature. Products were formed in up to 99% yield and 98 : 2 e.r. Using mechanistic and kinetic studies, including time course <sup>1</sup>H NMR monitoring, we revealed that the reaction likely proceeds *via* face-selective protonation of an enol-type intermediate.

## Introduction

The hydantoin scaffold exhibits a diverse array of bioactivities, for instance, phenytoin **1** is a well-known anti-seizure treatment, while enzalutamide **2** is a nonsteroidal antiandrogen used in the treatment of prostate cancer (Fig. 1).<sup>1</sup> Bioactive 5-monosubstituted hydantoins include, amongst others, the phenytoin analogue, ethotoin **3**, and the marine natural products agesamides A and B **4**<sup>2</sup> and parazoanthine A **5**.<sup>3</sup> Furthermore, enantioenriched 5-monosubstituted hydantoins serve as useful chiral auxiliaries in a variety of diastereoselective reactions.<sup>4–6</sup> The presence of various vectors for functionalisation of the hydantoin scaffold, along with the sp<sup>3</sup>-hybridised stereocentre, renders them useful for investigation as “3D” fragments in early-stage drug discovery.<sup>7</sup> Despite their importance, however, there are relatively few methods available for the asymmetric synthesis of 5-monosubstituted hydantoins from achiral precursors (Fig. 2a–c).

One effective strategy for enantioselective synthesis of 5-monosubstituted hydantoins is the asymmetric hydrogenation of prochiral hydantoins **6** bearing exocyclic alkenes at the 5-position (Fig. 2a). This type of approach was first reported by Takeuchi in 1987,<sup>8</sup> who used a Co catalyst in the presence of an amine ligand to prepare enantioenriched hydantoins **7** in up to 82% ee. More recently, precious metal catalysts have

been used to effect the same overall transformation in the presence of chiral phosphine ligands, including Pd<sup>9</sup> (up to: 96% yield; 90% ee), Rh<sup>10</sup> (up to: 99% yield; 97% ee), and Ir<sup>11</sup> (up to: 99% yield; 98% ee). A limitation of this strategy is that it can only deliver hydantoins bearing aliphatic substituents at the 5-position.

Building upon an earlier protocol by Shi,<sup>12</sup> in 2018 Gong reported the enantioselective  $\alpha$ -amination of pentafluorophenyl esters **8** using diaziridinone **9**, mediated by cooperative catalysis between Cu(i) and the chiral benzotetramisole catalyst **10** (Fig. 2b).<sup>13</sup> The enantiodetermining step was postulated to proceed *via* face-selective attack of a urea-derived *N*-centred radical onto a chiral benzotetramisole-derived enamine intermediate. Some limitations of this approach are the need for pentafluorophenyl esters **8** to achieve high ee's, high catalyst (and ligand) loadings, and the use of superheated solvent.

In 2021, Bach introduced an elegant photochemical deracemisation of hydantoins **11** mediated by hydrogen atom transfer in the presence of a chiral diarylketone **12** (Fig. 2c).<sup>14,15</sup>

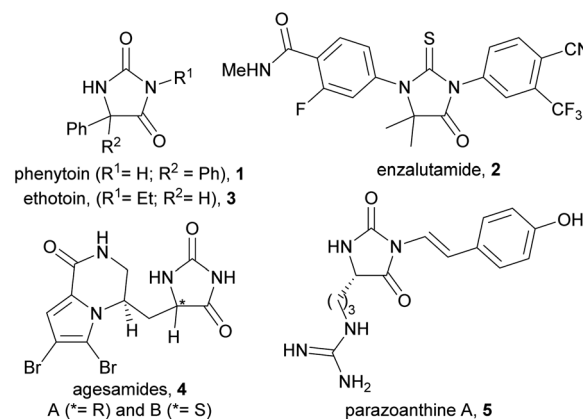


Fig. 1 Examples of bioactive hydantoins.

<sup>a</sup>School of Physical and Chemical Sciences, University of Canterbury, Christchurch, New Zealand. E-mail: daniel.foley@canterbury.ac.nz

<sup>b</sup>Center for Continuous Flow Synthesis and Processing, Research Center Pharmaceutical Engineering, Graz, Austria

<sup>c</sup>Biomolecular Interaction Centre, University of Canterbury, Christchurch, New Zealand

† Electronic supplementary information (ESI) available: Compound **21a** was formed as a racemate. CCDC 2235705, 2235706, 2241398. For ESI and crystallographic data in CIF or other electronic format see DOI: <https://doi.org/10.1039/d3sc01656k>

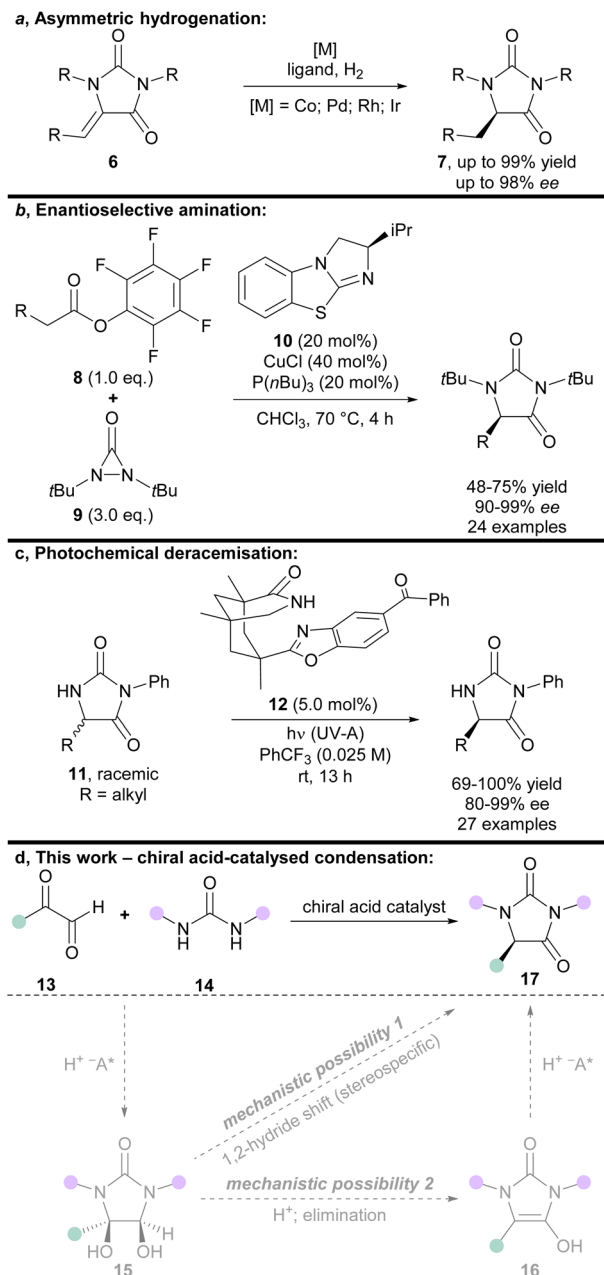


Fig. 2 (a–c) State-of-the-art methods for the asymmetric synthesis of hydantoin; (d) chiral acid-catalysed condensation of glyoxals and ureas (this work), including possible mechanisms for enantioinduction (grey arrows/structures).

Some constraints of the approach are that it appears limited to hydantoin that bear an irremovable *N*-phenyl group at the 3-position, and aliphatic groups at the 5-position. It also requires a fluorinated solvent, and low reactant concentrations.

Given the demand for enantiopure hydantoin, the development of new methods for their asymmetric synthesis from easily accessible achiral precursors remains an important area of research. We envisioned that a new enantioselective synthesis of hydantoin could be achieved *via* chiral acid-catalysed condensation of glyoxals and ureas (Fig. 2d).

To the best of our knowledge, the acid-mediated condensation of arylglyoxals and ureas was first reported by Arnold and Möbius in the patent literature in 1970.<sup>16</sup> Prior to this, Ekeley and Ronzio had reported that the reaction was only successful under base-mediated conditions.<sup>17</sup> Despite being known for >80 years, both the acid- and base-mediated condensations of glyoxals and ureas have received relatively little attention, with <150 reports in SciFinder to date. Significantly, none of the reported condensations of substituted glyoxals and ureas in the literature are enantioselective.

The acid-mediated condensation of substituted glyoxals **13** and ureas **14** has been suggested<sup>18,19</sup> to occur *via* a reaction mechanism related to that established for the Biltz hydantoin synthesis from 1,2-diketones and ureas (Fig. 2d, mechanistic possibility 1).<sup>20</sup> In this mechanism, glyoxals **13** and ureas **14** would first react to form vicinal diol intermediates **15**, which would then undergo 1,2-hydride migration (presumably in a stereospecific manner).<sup>18,19</sup> Vicinal diol intermediates **15** have been isolated and fully characterised previously.<sup>21,22</sup> However, we envisioned that an alternative mechanism may be possible (Fig. 2d, mechanistic possibility 2); elimination of the vicinal diol intermediate **15** would afford planar enol-type intermediate **16**, which could then undergo protonation to provide the hydantoin product **17**.

Regardless of whether the reaction proceeds *via* mechanistic possibility 1 or 2 (Fig. 2d), we envisioned that use of an appropriate chiral acid could enable an asymmetric condensation to give hydantoin **17**, either by (i) controlling face-selective addition of ureas **14** to glyoxals **13** to give enantioenriched diols **15** (followed by stereospecific 1,2-hydride migration); or (ii) by face-selective protonation of enols **16**.

Chiral phosphoric acids (CPAs) have proved immensely powerful for effecting asymmetric reactions in recent years, and are conveniently tuned because of their structural modularity and ease-of-synthesis.<sup>23–27</sup> We herein describe the first asymmetric synthesis of hydantoin from glyoxals and ureas, using chiral phosphoric acid catalysis.

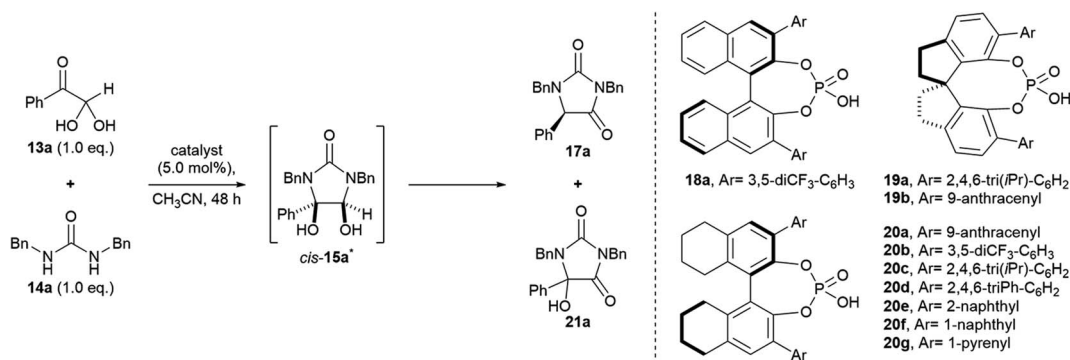
## Results and discussion

Our studies began by investigating the chiral phosphoric acid-catalysed condensation of phenylglyoxal monohydrate **13a** with 1,3-dibenzylurea **14a** in CH<sub>3</sub>CN at rt. The first reactions (entries 1–3, Table 1) were performed under air atmosphere and “ordinary” laboratory lighting (overhead 9 W white LEDs inside a fumehood). Initial investigations using (*R*)-BINOL and (*R*)-SPINOL-derived CPAs, **18a** and **19a**, resulted in complete conversion of the reactants to the hydantoin **17a**, but no enantiomeric enrichment of the product was observed (entries 1–2). Use of (*R*)-H<sub>8</sub>-BINOL **20a** (5.0 mol%), bearing 9-anthracenyl substituents at the 3 and 3′ positions, afforded the corresponding hydantoin **17a** in 40% isolated yield and 85 : 15 e.r., however, a major side product, 5-hydroxyhydantoin **21a** (32%) was also formed under the reaction conditions,\* as well as several other unidentified products (entry 3).

Carrying out the reaction using (*R*)-H<sub>8</sub>-BINOL **20a** in the absence of oxygen, and in the dark, provided the targeted



Table 1 Preliminary investigations and initial optimisations



Entry <sup>a</sup>	Catalyst	Conditions	Ratio 17a : 21a <sup>b</sup>	Isolated yield 17a/%	e.r. <sup>c</sup> 17a
1 <sup>d</sup>	<b>18a</b>	Air atmosphere, light <sup>h</sup>	100 : 0	98	52 : 48
2 <sup>e</sup>	<b>19a</b>	Air atmosphere, light	100 : 0	84	52 : 48
3	<b>20a</b>	Air atmosphere, light	55 : 45 <sup>f</sup>	40	85 : 15
4	<b>20a</b>	Ar atmosphere, dark	>99 : trace	98	85 : 15
5	<b>20b</b>	Ar atmosphere, light	100 : 0	99	62 : 38
6	<b>20c</b>	Ar atmosphere, light	100 : 0	nd <sup>g</sup>	50 : 49
7	<b>20d</b>	Ar atmosphere, light	100 : 0	98	70 : 30
8	<b>20e</b>	Ar atmosphere, light	100 : 0	98	72 : 28
9	<b>20f</b>	Ar atmosphere, light	100 : 0	98	81 : 19
10	<b>20g</b>	Ar atmosphere, light	100 : 0	98	80 : 20
11	<b>19b</b>	Ar atmosphere, dark	>99 : trace	98	29 : 71

<sup>a</sup> Unless indicated, the reaction conditions were: phenylglyoxal monohydrate **13a** (0.1 mmol), 1,3-dibenzylurea **14a** (0.1 mmol), catalyst (5.0 mol%), CH<sub>3</sub>CN (0.1 M), rt, no stirring, 48 h. <sup>b</sup> Ratio determined by analysis of the <sup>1</sup>H NMR spectra (600 MHz, CD<sub>3</sub>CN) before purification. <sup>c</sup> Determined by chiral HPLC (see ESI). <sup>d</sup> 24 h. <sup>e</sup> 36 h. <sup>f</sup> **21a** isolated in 32% yield. <sup>g</sup> 90 : 10 ratio of **15a** to **17a** by analysis of the <sup>1</sup>H NMR spectra (600 MHz, CD<sub>3</sub>CN). Nd = not determined. <sup>h</sup> Relative stereochemistry shown; major enantiomer unknown (see later). <sup>h</sup> Normal overhead fumehood lighting.

hydantoin **17a** in 98% isolated yield, and 85 : 15 e.r. (entry 4). Presumably, exposure to light (entry 3) leads to singlet oxygen formation *via* photosensitisation of triplet oxygen by the excited 9-anthracenyl rings on (*R*)-H<sub>8</sub>-BINOL **20a**. Singlet oxygen subsequently undergoes [2 + 2] cycloaddition with an enol intermediate of type **16**, resulting in the formation of 5-hydroxyhydantoin **21a** (Fig. S2<sup>†</sup>).<sup>28,29</sup> A <sup>1</sup>H NMR time course experiment over 48 h revealed >99% conversion to the target hydantoin **17a** when the reaction was carried out in the absence of oxygen and light; only a marginal trace of 5-hydroxyhydantoin **21a** formed (Fig. S1<sup>†</sup>). Interestingly, in the presence of oxygen, but the absence of light, the <sup>1</sup>H NMR ratio of **17a**:**21a** after 48 h was 94 : 6, suggesting that a slow background reaction between triplet oxygen and enol **16a** (Table S1, entry 6<sup>†</sup>).<sup>28,29</sup>

Our initial results (entries 1–4) suggested that (i) a H<sub>8</sub>-BINOL backbone, or (ii) large bulky substituents at the 3 and 3' positions, or (iii) both, were needed in order to prepare the hydantoin products in high e.r. To investigate these hypotheses, first the use of alternate CPAs based on H<sub>8</sub>-BINOL were explored in the reaction (entries 5–11). Notably, H<sub>8</sub>-BINOL catalysts bearing large fused aromatic rings at the 3 and 3' positions, *e.g.* 1-naphthyl and 1-pyrenyl rings (entries 9 and 10), provided the product in similar yields to (*R*)-H<sub>8</sub>-BINOL **20a** (entry 4) but did not improve upon the e.r. achieved (81 : 19 and 80 : 20 e.r., respectively, *vs.* 85 : 15 for **20a**). Secondly, the (*R*)-SPINOL CPA

**19b**, bearing a 9-anthracenyl substituent at the 6 and 6' positions was explored in the reaction (entry 11). This showed preference for the formation of the (*S*)-enantiomer of hydantoin **17a**, which was formed in 98% yield and 29 : 71 e.r. Since our investigations of the CPA structure did not furnish further improvements to the isolated yield and e.r. of the hydantoin product **17a**, we chose to proceed and investigate optimisation of other reaction parameters using the anthracenyl-substituted (*R*)-H<sub>8</sub>-BINOL **20a** catalyst.

We next chose to investigate the reaction solvent, which can markedly influence the solubility and relative acidity (pK<sub>a</sub>) of chiral phosphoric acids.<sup>30</sup> Conversion to hydantoin **17a** was highest in aprotic solvents (Table 2, entries 1–6), with complete conversion and the highest e.r.'s achieved in chlorinated solvents (entries 5–6), in which the catalyst was fully solubilised (*cf.* CH<sub>3</sub>CN). Most notably, when the reaction was run in CHCl<sub>3</sub> it proceeded to give hydantoin **17a** in 99% yield and 96 : 4 e.r. (entry 6). In contrast, in polar protic EtOH, conversion to hydantoin **17a** was sluggish, with *cis*-diol **15a** being the major component of the reaction mixture at 48 h (entry 7).

Investigation of the reaction in CHCl<sub>3</sub> using the other front-running catalysts, **20f** and **20g**, did not lead to improvements in the e.r. of the hydantoin **17a**, although the isolated yield essentially remained the same (entries 8–9). Further investigations therefore focused on optimising the



protocol using (*R*)-H<sub>8</sub>-BINOL **20a** as the catalyst. Lowering the catalyst **20a** loading to 2.0 mol% led to only slight erosion in e.r. (96 : 4 → 95 : 5), with 99% isolated yield, and the reaction was found to be complete at 20 h (entry 10). Further lowering of the catalyst **20a** loading led to unacceptable erosion of the e.r. and conversion in 48 h (entries 11–13). Heating the reaction to 60 °C reduced the reaction time to two hours, expediently providing hydantoin **17a** in 99% isolated yield and with slightly diminished e.r. (91 : 9, entry 14). To improve the e.r. of the product **17a**, the method in entry 14 may be coupled with recrystallisation (see below). When the reaction temperature was lowered to 0 °C (entry 15), the e.r. of hydantoin product **17a** was improved to 97 : 3, but at the expense of both reaction time (incomplete at 72 h) and isolated yield (96%). The presence of drying agents did not alter the enantioselectivity of the process (Table S2, entries 1–6; 8†). Addition of activated molecular sieves slowed the reaction down (entries 3–6; 8), however, addition of 10 eq. H<sub>2</sub>O had no effect on the yield, e.r., or reaction time (entry 7).

Based on the high yield and e.r. of hydantoin **17a** produced when 2.0 mol% (*R*)-H<sub>8</sub>-BINOL **20a** was used at room temperature for 20 h (entry 10), these conditions were chosen to explore the substrate scope.

Our optimised conditions (Table 2, entry 10) were directly applicable to a range of glyoxal (and glyoxal hydrate) starting materials to prepare enantioenriched hydantoin (Scheme 1). Glyoxals bearing electron-rich (4-Me; 4-OH; 4-OMe; 4-Oph) and moderately electron deficient (4-F; 4-Cl; 4-Br; 4-I) aryl rings were well tolerated in the protocol, with all yields ≥96% and e.r.'s

≥90 : 10. Electron deficient 4-CF<sub>3</sub>- and 4-NO<sub>2</sub>-phenylglyoxal monohydrates, performed sluggishly in the reaction (→ **17j–k**), with incomplete conversion after seven days at rt. Analysis by <sup>1</sup>H NMR at 600 MHz revealed the ratio of *cis*-diol **15j** to hydantoin **17j** to be 38 : 62, while the ratio of **15k** to hydantoin **17k** was 35 : 65. Interestingly, heating these reactions to 60 °C gave complete conversion to hydantoins **17j–k** in just 4 h. Hydantoin **17j** was isolated in 98% yield and 90 : 10 e.r., while compound **17k** was isolated in 95% yield and 85 : 15 e.r.

Substituents at the aryl 3-position were well tolerated in the reaction. 3-OMe-phenylglyoxal hemihydrate gave hydantoin **17l** in 96% yield and 94 : 5 e.r., while 3-Cl-phenylglyoxal hemihydrate gave **17m** in 96% yield and 92 : 8 e.r. Electron deficient 3,4-(difluoro)phenylglyoxal monohydrate reacted to give hydantoin **17n** in 75% isolated yield and 93 : 7 e.r. at rt, although the reaction was incomplete at 72 h (the ratio of **15n** to **17n** was 23 : 77 when the crude reaction mixture was analysed by <sup>1</sup>H NMR at 600 MHz). At rt, the reaction only went to completion after five days, giving compound **17n** in 95% yield and 91 : 9 e.r. However, heating the reaction to 60 °C provided compound **17n** in 98% yield and 89 : 11 e.r. after 4 hours.

The reaction of sterically hindered 2-substituted arylglyoxals produced hydantoins with lower e.r.'s (→ **17o–q**; 64 : 36–79 : 21 e.r.), which was also observed in the case of 1-naphthylglyoxal hemihydrate (→ **17r**; 74 : 26 e.r.). However, reaction of the sterically less hindered 2-naphthylglyoxal monohydrate yielded **17s** in 96% yield and 94 : 6 e.r. Heteroaromatic 5-bromo-2-thiophenylglyoxal monohydrate gave **17t** in 97% yield and 91 : 9 e.r.

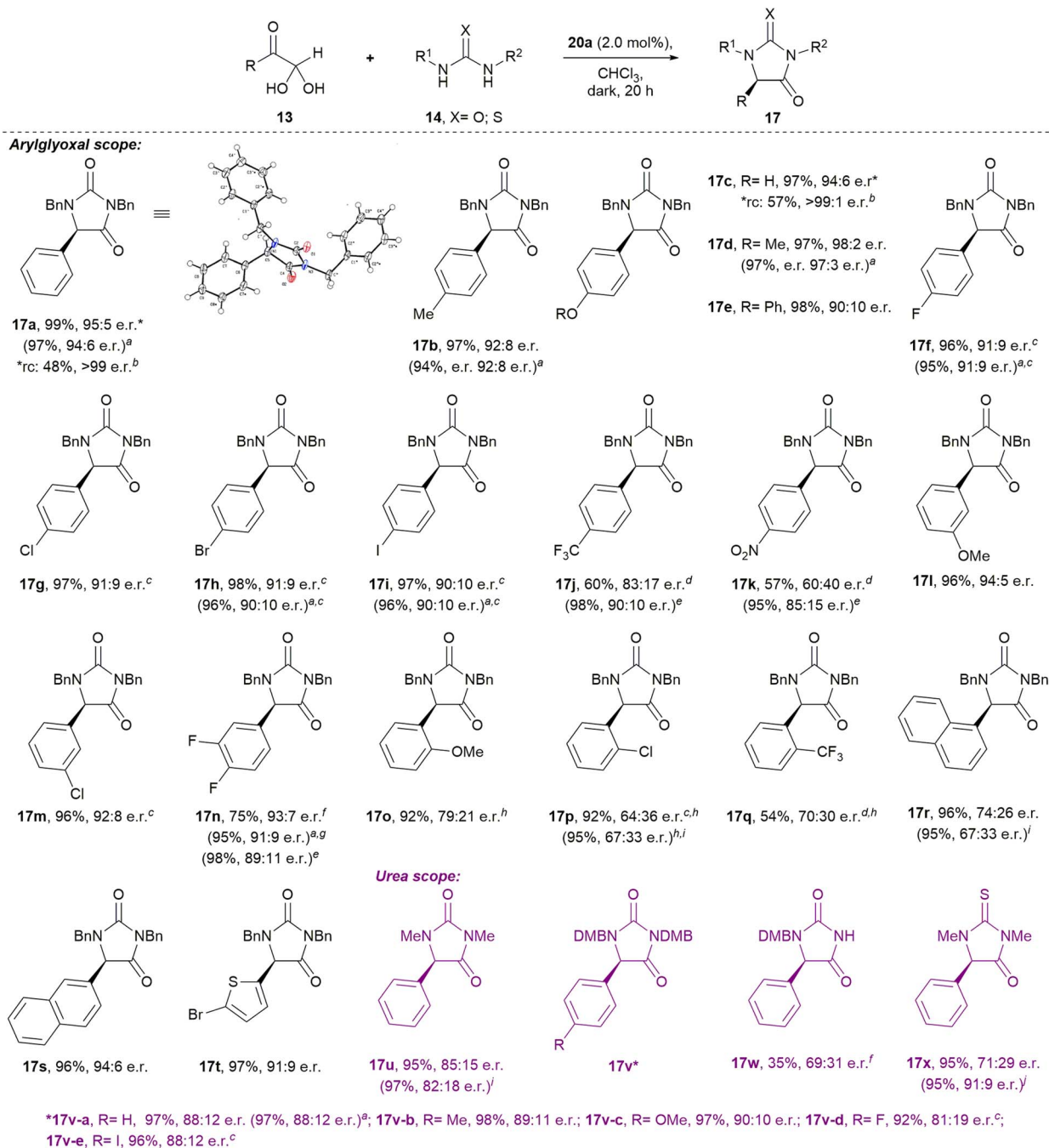
Table 2 Further optimisations

Reaction scheme showing the conversion of phenylglyoxal monohydrate (**13a**, 1.0 eq.) and 1,3-dibenzylurea (**14a**, 1.0 eq.) to hydantoin (**17a**) using a catalyst (5.0 mol%) in a solvent, dark, for 48 hours.

Entry <sup>a</sup>	Solvent	Catalyst (loading/mol%)	Ratio <b>15a</b> : <b>17a</b> <sup>b</sup>	Isolated yield <b>17a</b> /%	e.r. <b>17a</b> <sup>c</sup>
1	CH <sub>3</sub> CN	<b>20a</b>	0 : 100 <sup>d</sup>	98	85 : 15
2	Et <sub>2</sub> O	<b>20a</b>	28 : 72 <sup>d</sup>	71	81 : 19
3	THF	<b>20a</b>	40 : 60 <sup>d</sup>	60	76 : 26
4	PhMe	<b>20a</b>	16 : 84 <sup>d</sup>	84	86 : 14
5	CH <sub>2</sub> Cl <sub>2</sub>	<b>20a</b>	0 : 100	99	94 : 6
6	CHCl <sub>3</sub>	<b>20a</b>	0 : 100	99	96 : 4
7 <sup>e</sup>	EtOH	<b>20a</b>	55 : 29 <sup>df</sup>	29	69 : 31
8	CHCl <sub>3</sub>	<b>20f</b>	0 : 100	99	85 : 15
9	CHCl <sub>3</sub>	<b>20g</b>	0 : 100	99	84 : 16
10 <sup>g</sup>	CHCl <sub>3</sub>	<b>20a</b> (2.0)	0 : 100	99	95 : 5
11	CHCl <sub>3</sub>	<b>20a</b> (1.0)	0 : 100	98	87 : 13
12	CHCl <sub>3</sub>	<b>20a</b> (0.5)	trace:100	97	85 : 15
13	CHCl <sub>3</sub>	<b>20a</b> (0.1)	10 : 90	90	66 : 34
14 <sup>h</sup>	CHCl <sub>3</sub>	<b>20a</b> (2.0)	0 : 100	99	91 : 9
15 <sup>i</sup>	CHCl <sub>3</sub>	<b>20a</b> (2.0)	4 : 96	96	97 : 3

<sup>a</sup> Unless indicated, the reaction conditions were: phenylglyoxal monohydrate **13a** (0.1 mmol), 1,3-dibenzylurea **14a** (0.1 mmol), catalyst (5.0 mol%), solvent (0.1 M), dark, Ar, rt, no stirring, 48 h. <sup>b</sup> Unless indicated, ratio determined by analysis of the <sup>1</sup>H NMR spectra (600 MHz, K<sub>2</sub>CO<sub>3</sub>-neutralised CDCl<sub>3</sub>) before purification. <sup>c</sup> Determined by chiral HPLC (see ESI). <sup>d</sup> Ratio determined by analysis of the <sup>1</sup>H NMR spectra (600 MHz, CD<sub>3</sub>CN) before purification. <sup>e</sup> 40 °C. <sup>f</sup> 16 : 55 : 29 ratio of **14a** : **15a** : **17a**. <sup>g</sup> 20 h. <sup>h</sup> 60 °C, 2 h. <sup>i</sup> 0 °C, 72 h.





**Scheme 1** Phosphoric acid-catalysed condensation of arylglyoxals with ureas to give enantioenriched hydantoin. Standard reaction conditions: **13** (0.1 mmol), **14** (0.1 mmol), catalyst **20a** (2.0 mol%), CHCl<sub>3</sub>, dark, Ar, rt, no stirring, NMR tube. (a) Scaled-up reaction conditions: **13** (0.5 mmol), **14** (0.5 mmol), catalyst **20a** (2.0 mol%), CHCl<sub>3</sub>, dark, Ar, rt, stirring, glass vial; (b) yield and e.r. after recrystallisation; (c) 40 h; (d) 7 days; (e) 60 °C, 4 h; (f) 72 h; (g) 5 days; (h) **13** (0.15 mmol) used; (i) 60 °C, 2 h; (j) 0 °C, 72 h; (k) 60 °C, 0.5 h. rc = recrystallisation (unoptimised) of the sample marked with an asterisk. DMB = 2,4-dimethoxybenzyl.

It is noteworthy that recrystallisation of the hydantoin products **17** could improve their e.r., for instance for **17a** and **17c**, in each case recrystallisation improved the e.r. to >99: trace. Additionally, the absolute configurations of hydantoin **17a**, **17f**, and **17h** were determined through single-crystal X-ray diffraction (see ESI†).

Excitingly, preliminary studies with alkylglyoxals demonstrated that the corresponding hydantoin **S17y-ac** can be prepared enantioselectively, albeit that further optimisation is required in future (see Scheme S1†).

Brief investigation of the urea component revealed that high yields and reasonable e.r.'s are maintained when 1,3-dimethylurea ( $\rightarrow$  **17u**) and 1,3-diDMB-urea were used in the protocol ( $\rightarrow$  **17v**).



Interestingly, 1-DMB-urea performed sluggishly in the reaction, but regioselectively provided the 1-protected hydantoin **17w** in 35% yield and 69:31 e.r. after 72 h (incomplete conversion). When 1,3-dimethylthiourea was reacted with phenylglyoxal monohydrate at rt, thiohydantoin **17x** was isolated in 95% yield and 71:29 e.r. When the reaction temperature was dropped to 0 °C, conversion to the thiohydantoin **17x** was incomplete after 72 h (the ratio of *cis*-diol **15x** to thiohydantoin **17x** was 11:89), and thiohydantoin **17x** was isolated in 86% yield and 62:38 e.r. Curiously, however, heating the reaction to 60 °C for 0.5 h gave thiohydantoin **17x** in 95% yield and 91:9 e.r.

Time course  $^1\text{H}$  NMR studies were used to investigate the kinetics of the condensation reaction in  $\text{CDCl}_3$  over 24 hours, both in the presence and absence of catalyst **20a**. A global optimisation algorithm was used to determine the two rate constants within the model by maximising the convergence of the model-predicted reaction outcomes to the experimental data (Fig. 3a, i-iii). In the absence of catalyst **20a**, the reaction between phenylglyoxal monohydrate and 1,3-dibenzylurea proceeded to make *cis*-diol **15a**, which barely reacted further (Fig. 3a-i). The first step was fitted as a second-order process, and the intramolecular cyclisation as a first-order process, to obtain rate constants of  $4.9 \text{ M}^{-1} \text{ h}^{-1}$  and  $0.0020 \text{ h}^{-1}$ , respectively. However, with the addition of 2.0 mol% (*R*)- $\text{H}_8$ -BINOL **20a**, both of these steps were considerably faster (Fig. 3a-ii). Second-order formation of the *cis*-diol **15a** proceeded with a rate of  $150 \text{ M}^{-1} \text{ h}^{-1}$ . Interestingly, the subsequent formation of hydantoin **17a** in the rate-determining step displayed linear (zero-order) behaviour with a fitted rate constant of  $0.0070 \text{ M h}^{-1}$ . By using the variable time normalisation analysis (VTNA) technique,<sup>31</sup> we graphically fitted the kinetic plot for the (*R*)- $\text{H}_8$ -BINOL **20a**-catalysed reaction with an 'artificial zero' after full conversion of the starting materials (from 5 h), and at a known concentration for intermediate **15a**. Subsequently, reaction of intermediate **15a** to form the corresponding product **17a** in the rate-determining step could be fitted with increased accuracy (rate constant =  $0.0067 \text{ M h}^{-1}$ ; and  $R^2 = 0.995$ , Fig. 3a-iii). This behaviour switched to first-order when **15a** was nearly consumed (see Fig. S13†). Future studies will endeavour to gain a deeper kinetic insight into the reaction system using approaches outlined by others.<sup>32-35</sup>

To gain a deeper understanding of the reaction mechanism, a series of experiments were carried out (Fig. 3b). First, we prepared and isolated racemic *cis*-diol **15a** (see ESI†) and then exposed it to the optimised reaction conditions (Fig. 3b-i). We obtained the corresponding hydantoin **17a** in 95:5 e.r., which is consistent with the e.r. obtained for the reaction between phenylglyoxal monohydrate and 1,3-dibenzylurea under the same conditions (*cf.* Scheme 1).

Secondly, we reacted phenylglyoxal monohydrate with 1,3-dibenzylurea in the presence of (*R*)- $\text{H}_8$ -BINOL **20a** for 1 hour at rt to afford *cis*-diol **15a** in 62% yield and 66:34 e.r. (see ESI†). When this scalemic *cis*-diol **15a** was treated with (achiral) diphenylphosphoric acid, hydantoin **17a** was isolated as a racemate (Fig. 3b-ii).

Finally, exposing racemic hydantoin **17a** to (*R*)- $\text{H}_8$ -BINOL **20a** for 48 hours resulted in recovery of racemic **17a** (Fig. 3b-iii).

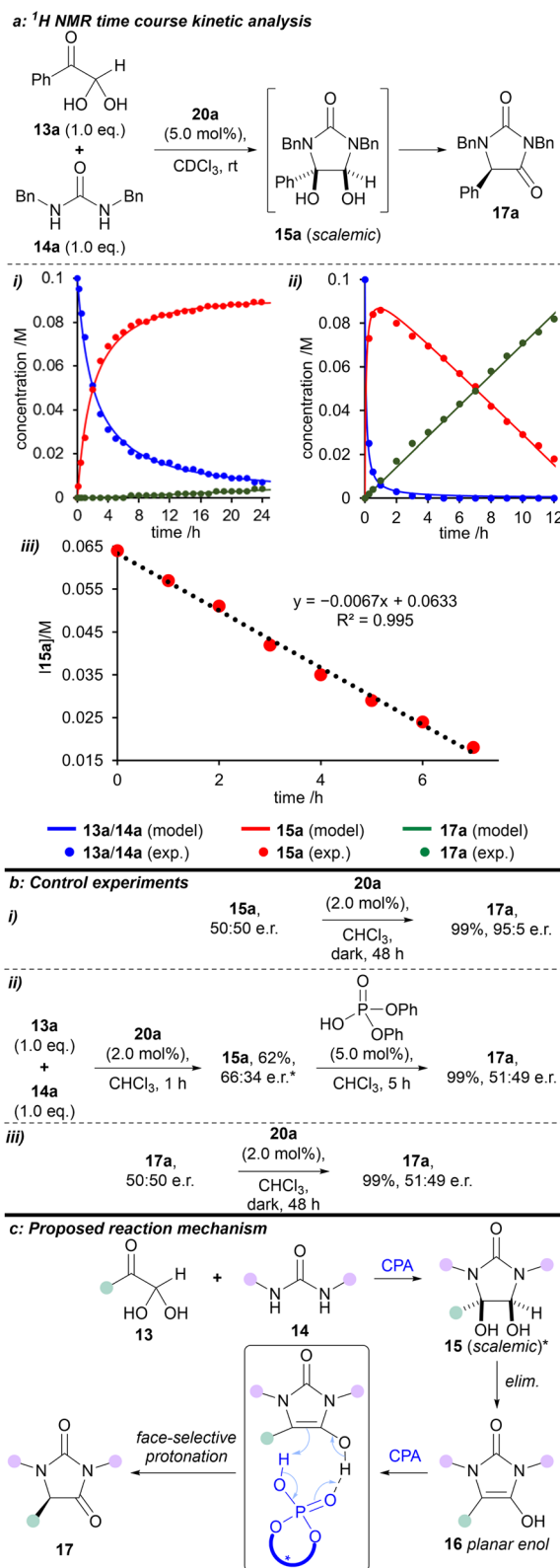
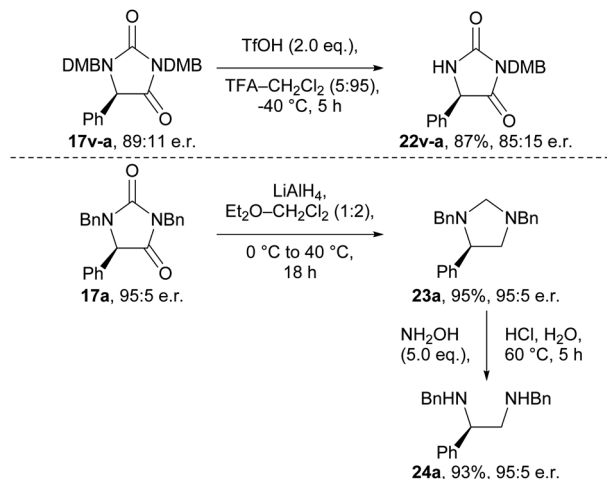


Fig. 3 Kinetic and mechanistic studies. (a)  $^1\text{H}$  NMR-derived time course kinetic analysis of the reaction between phenylglyoxal monohydrate **13a** and 1,3-dibenzylurea **14a** in  $\text{CDCl}_3$  at rt (600 MHz): (i) Reaction progress without catalyst; (ii) Reaction progress with catalyst **20a**; (iii) Variable time normalisation analysis (VTNA) concentration results against time with catalyst **20a**. (b) Control experiments. (c) Proposed reaction mechanism. \*Relative stereochemistry shown; major enantiomer unknown. exp. = experimental. elim. = elimination.





Scheme 2 Synthetic modification of the enantioenriched hydantoin.

Based on the above kinetic and experimental observations, we can explain the origin of enantioselectivity in the reaction (*R*)-H<sub>8</sub>-BINOL **20a** catalyses formation of (scalemic) *cis*-diol **15** then, in the enantiodetermining step, converts *cis*-diol **15** to enantioenriched hydantoin **17**, presumably *via* face-selective protonation of a transient, planar enol-type intermediate **16** (Fig. 3c). Further support for the reaction mechanism proceeding through a planar enol intermediate **16** is provided by the observed formation of 5-hydroxyhydantoin **21a** when the reaction is performed in the presence of singlet (and to a lesser extent triplet) oxygen.

To demonstrate the utility of the hydantoin products formed, we briefly investigated their synthetic modification to provide various chiral building blocks (Scheme 2). Our attempts to remove the *N*-benzyl groups *via* hydrogenation and other conditions were unfortunately unsuccessful (Tables S17 and S18<sup>†</sup>). However, we were able to remove the 2,4-dimethoxybenzyl (DMB) group from *N*-1 of hydantoin **17v-a** using TfOH at  $-40$  °C to give compound **22v-a**, albeit with some erosion in e.r. (89 : 11  $\rightarrow$  85 : 15). Additionally, we were able to obtain imidazolidine **23a** in 95% yield, and with complete retention of e.r., by reduction of enantioenriched hydantoin **17a** using LiAlH<sub>4</sub>.<sup>36</sup> Subsequent treatment of imidazolidine **23a** with hydroxylamine revealed vicinal diamine **24a**, a ligand scaffold used in enantioselective metal-catalysed reactions.<sup>37,38</sup>

## Conclusions

In summary, we have established a new asymmetric synthesis of hydantoins *via* the chiral phosphoric acid-catalysed condensation of glyoxals and ureas at room temperature. The reaction proceeds in high yields and enantioselectivities using a variety of substituted aryl glyoxals. Mechanistic investigations revealed that the enantiodetermining step likely arises from the face-selective protonation of a transient enol-type intermediate. Further development of this approach, for instance by modular structural variation of the chiral phosphoric acid catalyst, holds great promise for the broad application of this strategy in the enantioselective synthesis of hydantoins.

## Data availability

The relevant data is detailed in the ESI.<sup>†</sup>

## Author contributions

DJF conceptualised the idea and supervised the experimental work. SA completed all of the experimental work (except XRD). CH analysed the <sup>1</sup>H NMR time course studies carried out by SA, and derived the reaction rates. MIJP determined the crystal structures and absolute configurations of **17a**, **17f**, and **17h** by XRD. All authors contributed to writing the paper and ESI.<sup>†</sup>

## Conflicts of interest

There are no conflicts to declare.

## Acknowledgements

We thank the University of Canterbury (UC) and the Biomolecular Interaction Centre for funding. We thank UC for a Doctoral Scholarship for SA. We thank Alexis Blackie for her early contributions to our non-asymmetric study, which will be published in due course. We thank A/Prof. C. Fitchett for use of his normal-phase chiral HPLC column, A/Prof. V. Golovko for training SA to use the hydrogenation kit, and Dr M. Squire for set up of the NMR kinetic experiments.

## Notes and references

- L. Konnert, F. Lamaty, J. Martinez and E. Colacino, *Chem. Rev.*, 2017, **117**, 13757–13809.
- M. Tsuda, T. Yasuda, E. Fukushi, J. Kawabata, M. Sekiguchi, J. Fromont and J. Kobayashi, *Org. Lett.*, 2006, **8**, 4235–4238.
- N. Cachet, G. Genta-Jouve, E. L. Regalado, R. Mokrini, P. Amade, G. Culioli and O. P. Thomas, *J. Nat. Prod.*, 2009, **72**, 1612–1615.
- J. I. Yamaguchi, M. Harada, T. Narushima, A. Saitoh, K. Nozaki and T. Suyama, *Tetrahedron Lett.*, 2005, **46**, 6411–6415.
- J. S. Zhang, C. F. Lu, Z. X. Chen, Y. Li and G. C. Yang, *Tetrahedron: Asymmetry*, 2012, **23**, 72–75.
- X. R. Li, C. F. Lu, Z. X. Chen, Y. Li and G. C. Yang, *Tetrahedron: Asymmetry*, 2012, **23**, 1380–1384.
- A. Lutten, H. Gullberg, E. Abdurakhmanov, D. D. Vo, D. Akaberi, V. O. Talibov, N. Nekhotiaeva, L. Vangeel, S. De Jonghe, D. Jochmans, J. Krambrich, A. Tas, B. Lundgren, Y. Gravenfors, A. J. Craig, Y. Atilaw, A. Sandström, L. W. K. Moodie, Å. Lundkvist, M. J. van Hemert, J. Neyts, J. Lennerstrand, J. Kihlberg, K. Sandberg, U. H. Danielson and J. Carlsson, *J. Am. Chem. Soc.*, 2022, **144**, 2905–2920.
- S. Takeuchi and Y. Ohgo, *Bull. Chem. Soc. Jpn.*, 1987, **60**, 1449–1455.
- B. De Ma, S. H. Du, Y. Wang, X. M. Ou, M. Z. Huang, L. X. Wang and X. G. Wang, *Tetrahedron: Asymmetry*, 2017, **28**, 47–53.



- 10 G. Xiao, S. Xu, C. Xie, G. Zi, W. Ye, Z. Zhou, G. Hou and Z. Zhang, *Org. Lett.*, 2021, **23**, 5738.
- 11 Y. Nie, J. Li, Q. Yuan and W. Zhang, *Chin. J. Chem.*, 2022, **40**, 819–824.
- 12 B. Zhao, H. Du and Y. Shi, *J. Am. Chem. Soc.*, 2008, **130**, 7220–7221.
- 13 J. Song, Z. J. Zhang, S. Sen Chen, T. Fan and L. Z. Gong, *J. Am. Chem. Soc.*, 2018, **140**, 3177–3180.
- 14 J. Großkopf, M. Plaza, A. Seitz, S. Breitenlechner, G. Storch and T. Bach, *J. Am. Chem. Soc.*, 2021, **143**, 21241–21245.
- 15 R. J. Kutta, J. Großkopf, N. van Staalduinen, A. Seitz, P. Pracht, S. Breitenlechner, C. Bannwarth, P. Nuernberger and T. Bach, *J. Am. Chem. Soc.*, 2023, **145**, 2354–2363.
- 16 K. Arnold and G. Möbius, East Ger. Patent, DD89,846, 1972.
- 17 H. J. Fisher, J. B. Ekeley and A. R. Ronzio, *J. Am. Chem. Soc.*, 1942, **64**, 1434–1436.
- 18 V. G. Shtamburg, V. V. Shtamburg, A. A. Anishchenko, R. I. Zubatyuk, A. V. Mazepa, E. A. Klotz, S. V. Kravchenko and R. G. Kostyanovsky, *Chem. Heterocycl. Compd.*, 2015, **51**, 553–559.
- 19 V. G. Shtamburg, A. A. Anishchenko, V. V. Shtamburg, A. V. Mazepa, S. V. Kravchenko and E. A. Klots, *Eur. Chem. Bull.*, 2017, **6**, 215.
- 20 A. R. Butler and E. Leitch, *J. Chem. Soc., Perkin Trans. 2*, 1977, 1972–1976.
- 21 T. L. Hough, I. R. Hough and R. W. Pannell, *J. Heterocycl. Chem.*, 1986, **23**, 1125–1130.
- 22 V. G. Shtamburg, V. V. Shtamburg, A. A. Anishchenko, A. V. Mazepa and E. B. Rusanov, *J. Mol. Struct.*, 2022, **1264**, 133259.
- 23 T. Akiyama, J. Itoh, K. Yokota, K. Fuchibe, T. Akiyama, J. Itoh, K. Yokota and K. Fuchibe, *Angew. Chem., Int. Ed.*, 2004, **43**, 1566–1568.
- 24 D. Uraguchi and M. Terada, *J. Am. Chem. Soc.*, 2004, **126**, 5356–5357.
- 25 T. Akiyama, *Chem. Rev.*, 2007, **107**, 5744–5758.
- 26 M. Terada, *Chem. Commun.*, 2008, 4097–4112.
- 27 D. Parmar, E. Sugiono, S. Raja and M. Rueping, *Chem. Rev.*, 2014, **114**, 9047–9153.
- 28 A. F. Olea and F. Wilkinson, *J. Phys. Chem.*, 1995, **99**, 4518–4524.
- 29 H. H. Wasserman and S. Terao, *Tetrahedron Lett.*, 1975, **16**, 1735–1738.
- 30 K. Kaupmees, N. Tolstoluzhsky, S. Raja, M. Rueping and I. Leito, *Angew. Chem., Int. Ed.*, 2013, **52**, 11569–11572.
- 31 J. Burés, *Angew. Chem., Int. Ed.*, 2016, **55**, 16084–16087.
- 32 D. G. Blackmond, *Angew. Chem., Int. Ed.*, 2005, **44**, 4302–4320.
- 33 D. G. Blackmond, *J. Am. Chem. Soc.*, 2015, **137**, 10852–10866.
- 34 Z. Zhang, M. Klussmann and B. List, *Synlett*, 2020, **31**, 1593–1597.
- 35 Z. Zhang, Y. Liu, Z. Wang and K. Ding, *Asian J. Org. Chem.*, 2022, **11**, e202100795.
- 36 S. Cortes and H. Kohn, *J. Org. Chem.*, 1983, **48**, 2246–2254.
- 37 D. Lucet, T. Le Gall and C. Mioskowski, *Angew. Chem., Int. Ed.*, 1998, **37**, 2580–2627.
- 38 J. C. Kizirian, *Chem. Rev.*, 2008, **108**, 140–205.

